Nanoprecipitation-assisted ion current oscillations

MATTHEW R. POWELL[1], MICHAEL SULLIVAN[1], IVAN VLASSIOUK[1], DRAGOS CONSTANTIN[1], OLIVIER SUDRE[2], CRAIG C. MARTENS[3], ROBERT S. EISENBERG[4] AND ZUZANNA S. SIWY[1]*

[1]Department of Physics and Astronomy, University of California, Irvine, California 92697, USA
[2]Teledyne Scientific Co., 1049 Camino Dos Rios, Thousand Oaks, California 91360, USA
[3]Department of Chemistry, University of California, Irvine, California 92697, USA
[4]Rush Medical College, Department of Molecular Biophysics & Physiology, Chicago, Illinois 60612, USA
*e-mail: zsiwy@uci.edu

Published online: 23 December 2007; doi:10.1038/nnano.2007.420

Nanoscale pores exhibit transport properties that are not seen in micrometre-scale pores, such as increased ionic concentrations inside the pore relative to the bulk solution, ionic selectivity and ionic rectification. These nanoscale effects are all caused by the presence of permanent surface charges on the walls of the pore. Here we report a new phenomenon in which the addition of small amounts of divalent cations to a buffered monovalent ionic solution results in an oscillating ionic current through a conical nanopore. This behaviour is caused by the transient formation and redissolution of nanoprecipitates, which temporarily block the ionic current through the pore. The frequency and character of ionic current instabilities are regulated by the potential across the membrane and the chemistry of the precipitate. We discuss how oscillating nanopores could be used as model systems for studying nonlinear electrochemical processes and the early stages of crystallization in sub-femtolitre volumes. Such nanopore systems might also form the basis for a stochastic sensor.

Channels and pores in biological cells control almost every physiological function of living organisms[1]. Nanopores act as valves for ions, much as diodes and transistors act as valves for electrons and holes. Both also use tiny amounts of charge to control macroscopic flows[2,3]. Both synthetic and biological nanopores have begun to play an important role in biotechnology as sensors for viruses, DNA, proteins and other molecules[4–8]. Nanopores offer a suitable environment to design sensors with low detection limits, to study the behaviour of molecules in sub-femtolitre volumes, and to give insight into the fundamental science of interactions of ions and charged molecules at the nanoscale[9–11].

The transport properties of nanopores differ greatly from those of micrometre-sized pores because the increased surface-to-volume ratio in nanopores causes ions and molecules passing through the nanopore to be strongly influenced by the properties of the pore walls. In particular, charged pore walls result in the accumulation of counter-ions and the exclusion of co-ions near the surface[12,13]. Ionic concentrations are also strongly influenced by the applied transmembrane potential[14]. The combination of these two effects leads to large ionic gradients from inside the pore to the bulk electrolyte solution. These gradients play an important role in physiological processes and methods to enhance ionic fluxes in ionic diodes and transistors[1,2,15–18].

We show that the increased concentration of divalent cations near negatively charged pore walls of single conical nanopores prepared by the track-etching technique[19,20] can lead to the formation of transient precipitates and, as a result, to transient blockages of the ionic current. In our experiments, a membrane with a single conical nanopore (with its narrow opening measuring between 2 and 6 nm in diameter) was immersed in a solution containing 0.1 M KCl and various divalent ion salts at sub-millimolar concentrations, ensuring salt or hydroxide solubility in the bulk electrolyte. Inside the nanopore, the negative surface charges of the carboxyl groups created during the fabrication process[20] and the applied transmembrane potential increase the concentration of all the ions so the formation of precipitates is possible (Fig. 1a). Nanoprecipitates form even if ionic activities in the bulk solution are below the bulk solubility product K_{sp}. The formation of precipitate is observed as a voltage-dependent blockage of the ion current passing through the nanopore. Once the pore is closed, a new ion distribution is set up inside the pore, leading to the re-dissolution of the precipitate and reactivation of the ionic current. The few molecules in the precipitate control a macroscopic flow of current.

The blockage of current leads to two effects in the transport properties of single nanopores, which have been reported previously, but have not yet been fully explained: (1) negative incremental resistance (NIR) in current–voltage curves[21]; and (2) oscillations of ion current in time[22]. In a previous report[22] we indicated the importance of divalent ion adsorption on the pore walls to the occurrence of NIR. Here we provide experimental studies and theoretical modelling showing both the accumulation of divalent ions on the pore walls and the nanoprecipitation of cobalt and magnesium hydroxides along with calcium and cobalt hydrogen phosphates in the narrow opening of a conical nanopore. We discuss the dynamic character of nanoprecipitate formation, and its application in studying electrochemical oscillating systems and building biosensors, and in studying how nanocrystals seed the formation of macrocrystals.

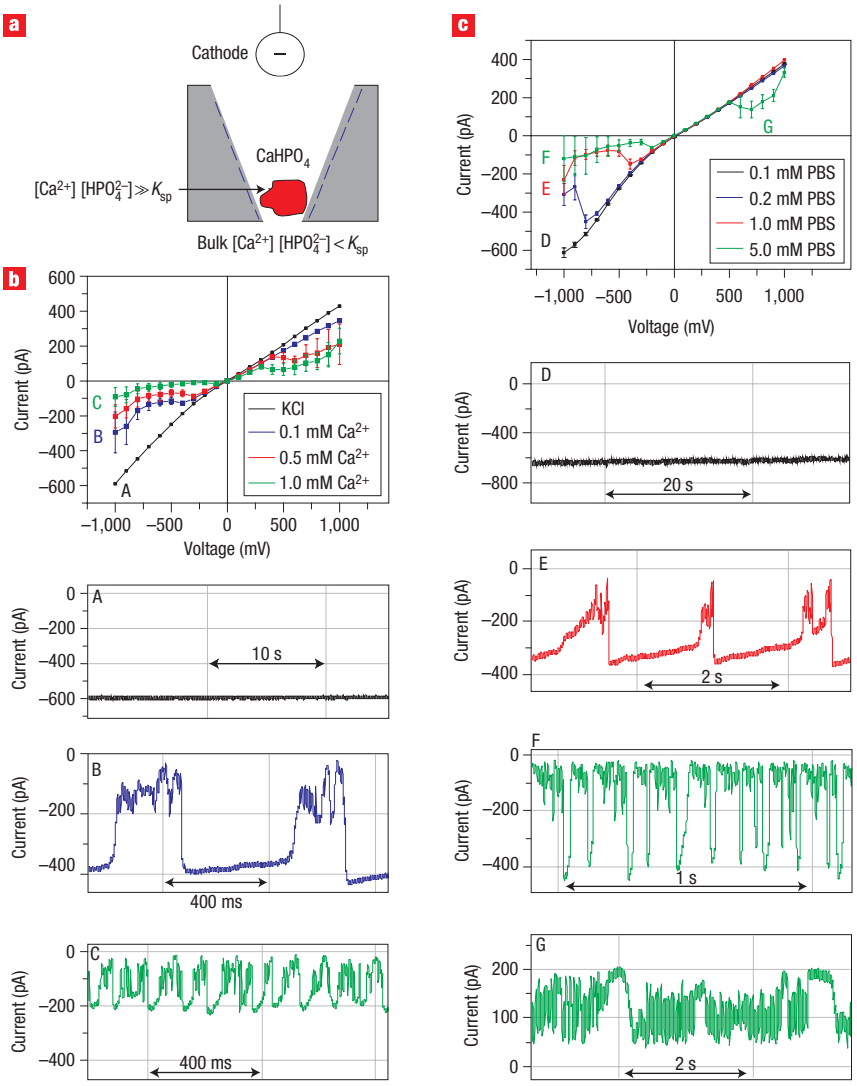

Figure 1 Nanoprecipitation of calcium hydrogen phosphate ($CaHPO_4$) in a single conical nanopore. a, When the negatively biased electrode (cathode) is at the larger opening of a conical nanopore, cations will move from the narrow opening towards the larger opening of the cone. The activities of Ca^{2+} and HPO_4^{2-} ions inside the nanopore with negative surface charges (blue dashed line) then rise above the solubility product K_{sp} of $CaHPO_4$, allowing nanoprecipitation to occur. In the bulk solution, the Ca^{2+} and HPO_4^{2-} activities remain below the value of K_{sp}. **b**, We studied a single conical nanopore with a tip opening of 2 nm diameter. Current–voltage curves and corresponding current signals versus time were recorded in 0.1 M KCl with 2 mM PBS buffer alone (black trace) and with varying calcium concentrations. A, B and C in the top panel relate to the traces in the lower panels. **c**, Current–voltage curves and corresponding current signals versus time (D–G) were recorded in 0.1 M KCl and 0.2 mM calcium with varying PBS concentrations, as indicated. Ion current time signals marked as A–F were recorded at −1,000 mV, and signal G was recorded at +700 mV. The colour of the signals corresponds to the colour of the *I–V* curves in **b** and **c**. Fluctuations of ion current were present mainly for negative voltages. Ion current instabilities were observed for positive voltages only for high Ca^{2+} and PBS concentrations for which the ionic activities in the bulk approached K_{sp}. For one recording shown in **b** performed in 0.1 M KCl, 1 mM $CaCl_2$ and 2 mM PBS (the green curve in **b**) the bulk ionic activities were above the value of K_{sp}. The error bars in the *I–V* curves indicate standard deviation.

NANOPRECIPITATION AND CURRENT INSTABILITIES

The first system in which nanoprecipitation was observed consisted of a single conical nanopore in polyethylene terephthalate (PET) in contact with a solution of 0.1 M KCl containing sub-millimolar concentrations of calcium, and buffered to pH 8 with 2 mM phosphate buffer (PBS). Figure 1b shows current–voltage (*I–V*) curves before and after adding calcium. Adding calcium in the presence of PBS induced a nonlinear behaviour in the *I–V* curve (NIR at negative voltages); that is, larger amplitudes of voltage induced smaller ionic fluxes[21].

We believe that the mechanism of NIR observed in our system involves the nanoprecipitation of calcium hydrogen phosphate ($CaHPO_4$) in the pore. The questions that then arise are 'How does the nanoprecipitation occur?' and 'How does the precipitate then dissolve to "reopen" the pore?' The phosphates in this system play the role of both buffer and reagent. Using 2 mM pH 8 PBS gives 1.9 mM hydrogen phosphate in the solution. Because of the significantly higher concentration of K_2HPO_4 we consider only $CaHPO_4$ precipitation. Moreover, the salt $Ca(H_2PO_4)_2$ is an easily soluble compound. The $CaHPO_4$ has a bulk solubility product K_{sp} of $\sim 1 \times 10^{-7}$ $[mol\,dm^{-3}]^2$ at ambient conditions[23].

For the typical calcium experiment that showed NIR, the product of these two activities is still below the solubility product, precluding any precipitation in the bulk electrolyte. However, the ion concentrations inside a nanopore with negative surface charges are very different from the values in the bulk solution[12,14,24,25]. The number of ions that dwell inside the pore at any time is also influenced by the applied transmembrane potential[14,24]; therefore the solubility product is expected to be exceeded only at a particular threshold potential. This is what was recorded experimentally, in that nanoprecipitates began to form above certain negative voltages, causing the formation of a 'plug' in the nanopore, and thus a decrease in the average ion current.

In order to support the hypothesis that nanoprecipitation is responsible for the NIR effect, we performed a series of measurements with 0.2 mM Ca^{2+} while varying the PBS buffer concentration (Fig. 1c). In both cases—that is, when varying either calcium or PBS concentration—the presence of calcium and phosphates predominantly affected the currents recorded for negative voltages. Currents recorded for positive voltages decreased only for very high bulk concentrations of calcium and PBS, at which the ionic activities approached K_{sp}.

The $I-V$ curves shown in Fig. 1 were obtained by averaging 30-s and 2-min recordings of ion currents in time. Large standard deviations recorded for high negative voltages indicate that the ion currents exhibit fluctuations of large amplitude. The lower panels of Fig. 1b,c show recordings of ion current versus time at −1,000 mV. For calcium and PBS concentrations where NIR was observed, the signals oscillated between a state of high ionic conductance and a state with a much smaller current. Interestingly, the frequency of oscillations was dependent on the bulk concentration of calcium and phosphate ions: for higher concentrations, the switching of the pore is more frequent (lower panels, Fig. 1b,c).

We were intrigued by the voltage-dependent behaviour of the ion current time series, and the occurrence of two-state switching of the ion current. We noticed that the voltage at which NIR occurs is also the voltage at which the ion current exhibits instabilities. This is clearly seen when comparing the power spectra of the following ion current recordings: (1) the time series for negative voltages that are below the threshold for NIR, (2) currents at voltages for which NIR has just commenced, and (3) recordings at −1,000 mV. Figure 2a shows the current time series together with histograms of the current values and Fig. 2b their power spectra in the frequency range 0.1–2,000 Hz. The signals at low negative voltages (−100 mV in Fig. 2) are indeed very 'quiet', which is confirmed by the low amplitudes in the power spectrum. At the voltage for which NIR has just started (−200 mV), the signal is much more 'noisy'; however, the pore stays predominantly in its low conductance state. The power spectrum amplitude of the time series at −200 mV is higher by several orders of magnitude compared to the recording at −100 mV. At −1,000 mV, regular bursts of the pore opening occur and are reflected in the power spectrum as a peak of frequency ∼10 Hz. This frequency indeed corresponds to the oscillations observed in the time series.

Figure 3a,b shows very similar results, with 0.1 M KCl containing various concentrations of $CoCl_2$ and 2 mM PBS. This time we observed fluctuations of ion current due to the formation of cobalt hydrogen phosphate precipitates ($CoHPO_4$), which had a bulk K_{sp} of $\sim 1 \times 10^{-7}$ $[\text{mol dm}^{-3}]^2$ (ref. 23). The observations in this system are qualitatively very similar to those with $CaHPO_4$. $I-V$ curves showed NIR, and ion current time series at high voltages exhibited a distinct two-state switching behaviour. The shape of the current oscillations deserves

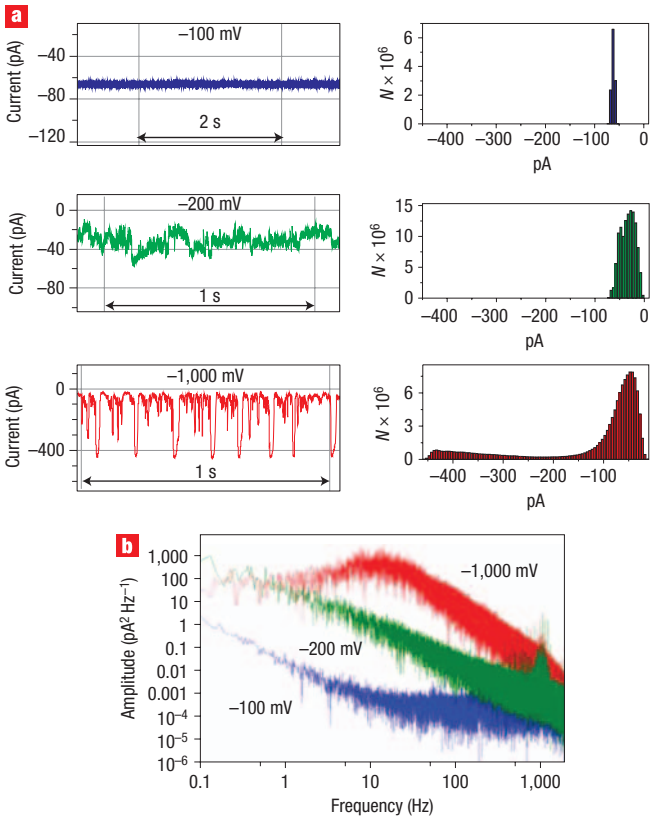

Figure 2 Ion current oscillations through a single conical nanopore induced by $CaHPO_4$ nanoprecipitates. **a**, Ion current time series along with current histograms for various applied voltages as indicated, with 0.1 M KCl, 0.2 mM $CaCl_2$ and 5 mM PBS. The data were recorded for the same pore as studied in Fig. 1. **b**, Power spectra of the ion current recordings shown in **a**. The peak between 10 Hz and 20 Hz for the −1,000 mV time series corresponds to oscillations of that frequency, which can be clearly seen from the time series.

attention. For $CoHPO_4$, the gradual decrease of ion current in time has, typically, a multistep character, indicative of damped oscillations (Fig. 3b). The timescale of the current oscillations can vary substantially for various pores. However, $CoHPO_4$-induced fluctuations typically have a lower frequency (∼1 Hz in Fig. 3c) than the $CaHPO_4$-induced fluctuations.

In order to provide further evidence for the role of nanoprecipitation in NIR and current instabilities, we experimented with nanoprecipitation for magnesium and cobalt hydroxides. These nanoprecipitation systems were chemically much simpler than those using hydrogen phosphates, because the anion participating in the precipitation was not a direct component of a buffer. The bulk K_{sp} of $Mg(OH)_2$ is 5.61×10^{-12} $[\text{mol dm}^{-3}]^3$ (ref. 23), but the bulk K_{sp} of $Co(OH)_2$ is significantly smaller at 5.92×10^{-15} $[\text{mol dm}^{-3}]^3$ (ref. 23). In experiments using magnesium ions, we expected to observe NIR for much higher concentrations than in experiments with cobalt ions. Figure 4a shows $I-V$ curves and Fig. 4b examples of ion currents in time for the system containing 0.1 M KCl, varying concentrations of $MgCl_2$ and pH 9.5. This system again showed a threshold of Mg^{2+} concentration at which the NIR effect occurred. Ion current oscillations in this case had a very low frequency, and the pore predominantly stayed in the low

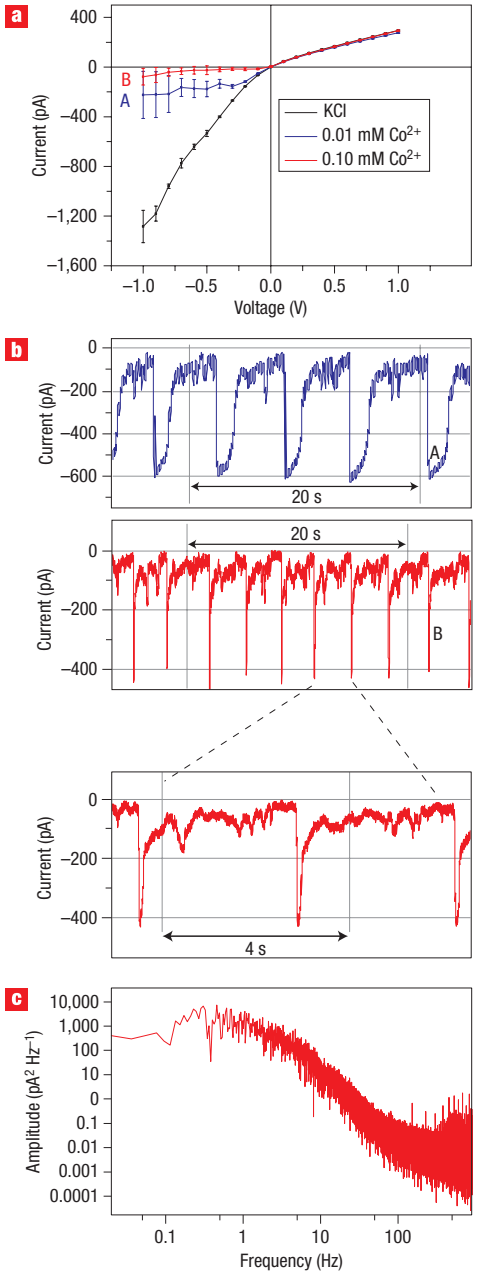

Figure 3 Nanoprecipitation of cobalt hydrogen phosphate ($CoHPO_4$) in a single nanopore. a, Current–voltage curves for 0.1 M KCl and 2 mM PBS buffer with varying cobalt salt concentrations. The tip opening of this pore was 6 nm in diameter. **b**, Time series recordings showing the details of $CoHPO_4$ oscillations at −1,000 mV for 0.01 mM (A) and 0.1 mM (B) cobalt ions. The colour of the signals corresponds to the colour of the *I*–*V* curves in **a**. **c**, Power spectra of ion current time series recorded in 0.1 mM Co^{2+}. A peak is visible for frequencies between 0.1 and 1 Hz corresponding to the brief open states occurring approximately every 3 s.

conductance state. (See Supplementary Information, Fig. S1, for the results for the $Co(OH)_2$ system.)

Further evidence for the nanoprecipitation hypothesis explaining NIR was provided by experiments performed with a complexing agent for polyvalent cations, ethylenediamine tetraacetic acid (EDTA). Adding EDTA caused the immediate disappearance of both the NIR and ion current instabilities (see Supplementary Information, Fig. S5).

EVIDENCE FOR NANOPRECIPITATION IN NANOPORES

The above-mentioned experiments provide evidence that weakly soluble compounds can precipitate inside a single nanopore that has negative surface charge.

The questions that have to be answered are as follows. Are the ionic concentrations sufficiently high to cause precipitation? Why do NIR and ion current oscillations occur predominantly for negative voltages? And why is the nanoprecipitate formation dynamic; that is, what produces its time course and its dissolution?

In order to answer the first two questions, we checked the precipitation conditions in our system by comparing the product of ionic activities in a conical nanopore with the solubility product K_{sp}. We used the specific interaction theory to calculate the activity coefficients of the ions[26,27] (see Supplementary Information). The ionic concentrations were modelled with the Poisson–Nernst–Planck (PNP) equations[28,29]. We considered a static case, and we modelled the ionic concentrations in a nanopore that is in contact with an electrolyte of a given composition. It is important to mention that we assumed that solubility products in the pore are the same as in the bulk K_{sp}. We are aware that the precipitation conditions inside nanopores, where the ratio of surface to volume is very large, might be different from the bulk. Inside nanopores, precipitation probably occurs for activity products that are smaller than K_{sp}.

Because of the small opening angle of our conical nanopores (~3°), the one-dimensional PNP model provides a very good qualitative and quantitative description of ion transport[24]. Figure 4c–e shows the product of ionic activities in the nanopore calculated for the $Mg(OH)_2$ system as a function of the position along the pore's axis and the transmembrane potential. These results confirm that the ionic activities inside the pore are strongly voltage dependent. For negative voltages above ~400 mV and Mg^{2+} concentration of 0.5 mM, the product of the predicted ionic activities significantly exceeds the K_{sp} value, thus enabling nanoprecipitation. For the range of negative voltages above ~500 mV, NIR was indeed observed experimentally (see the red curve in Fig. 4a).

The PNP modelling also explains why the precipitation is predominantly observed for negative voltages. The conical geometry of the nanopore is responsible for the asymmetric distributions of ionic concentrations at the two voltage polarities. For positive voltages, ionic concentrations at the tip of the pore are in fact smaller than in the bulk, therefore no precipitates of $Mg(OH)_2$ are formed (Fig. 4d).

The third important question remains: What is the mechanism behind the transient formation and dissolution of the nanoprecipitates? A simple explanation would be to assume that, once formed, the nanoprecipitate 'plug' gets pushed through the pore by the applied electric field. This explanation, however, does not account for the different timescales we see for different compounds at the moment when the pore is opening. We believe that the mechanism for precipitate dissolution is electrical in character (Fig. 5). When the pore is plugged with the nanoprecipitates, almost the entire voltage drop occurs on the precipitate. The electric field in the regions that are adjacent to the precipitate is therefore much lower, which in turn causes the ionic activities to decrease. As can be seen in Fig. 4e, decreasing the voltage from −500 mV to −100 mV changes the product of the ionic activities by several orders of magnitude. However, the electric field in this region is finite, which promotes the removal of cations from the pore. The concentration of ions also

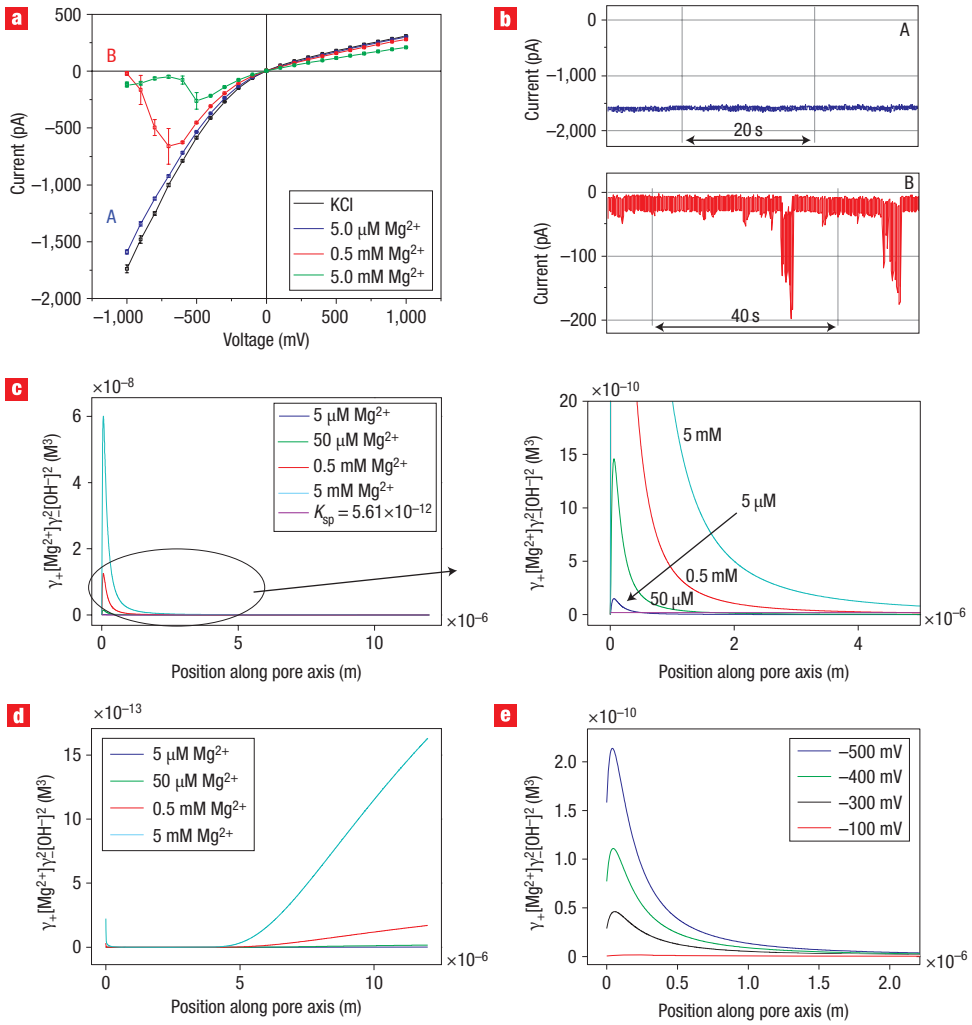

Figure 4 Nanoprecipitation of magnesium hydroxide ($Mg(OH)_2$) in a single nanopore. a, Current–voltage curves of a single nanopore for 0.1 M KCl and 2 mM CAPSO buffer at a pH of ~9.5 with varying magnesium concentrations. The tip opening of this pore was 5 nm in diameter. **b**, Time series of ion current recordings for 5 μM (A) and 500 μM (B) magnesium chloride at −1,000 mV. The colour of the signals corresponds to the colour of the *I*–*V* curves in **a**. **c**,**d**, Theoretical results from the one-dimensional Poisson–Nernst–Planck model mapping the products of the magnesium and hydroxide activities for −1,000 mV (**c**), +1,000 mV (**d**), along the pore axis. Position 0 corresponds to the tip of the pore. The modelling confirms that the ionic concentrations in the pore are very different for the two voltage polarities, so the nanoprecipitates form for negative voltages. **e**, Theoretical products of activities for 0.5 mM Mg in the bulk at various voltages (as indicated) showing the transmembrane-potential-dependent onset of nanoprecipitation. The nanopore that was modelled had opening diameters of 5 nm and 400 nm.

decreases due to the diffusion of ions out of the pore and into the bulk where concentrations are smaller. These effects work together to greatly decrease the local ionic concentrations, which promotes the dissolution of the precipitates. The pore is then open, ions can move freely, and the process of reforming the precipitates starts again. This scenario also explains why at voltages for which NIR commences, the current stays predominantly in its closed state. In this case the electric field is too low to create a depletion zone that would induce dissolving of the precipitate.

APPLICATION OF ELECTROCHEMICAL OSCILLATIONS

Electrochemical oscillations have attracted much scientific interest, largely because of oscillations observed in the physiological processes of living organisms as well as nonlinear chemical systems[30], such as the Bielousov-Zhabotinskii reaction[31]. The transient nanoprecipitation observed in our conical nanopores could serve as a model system for studying chemical oscillations of much higher frequencies than those observed in previously studied electrochemical oscillators. The high oscillating frequencies achieved in our system correspond to dynamic changes occurring in a sub-femtolitre volume of a single nanopore.

Our oscillating nanopore operates far from equilibrium and as such is very sensitive to changes in external parameters[32], such as the addition of a biomolecule to the solution. Figure 6a,b shows $CoHPO_4$-induced ion current oscillations before and after adding 15 μM neomycin. This small amount of neomycin, which at pH 8 is positively charged, caused an immediate disappearance of the characteristic current switching. Interestingly, adding another positively charged molecule, spermine, had a different effect, in that the frequency of the ion current oscillations increased (Fig. 6c,d). It is important to mention that the molecules could not be detected without the nanoprecipitation reaction;

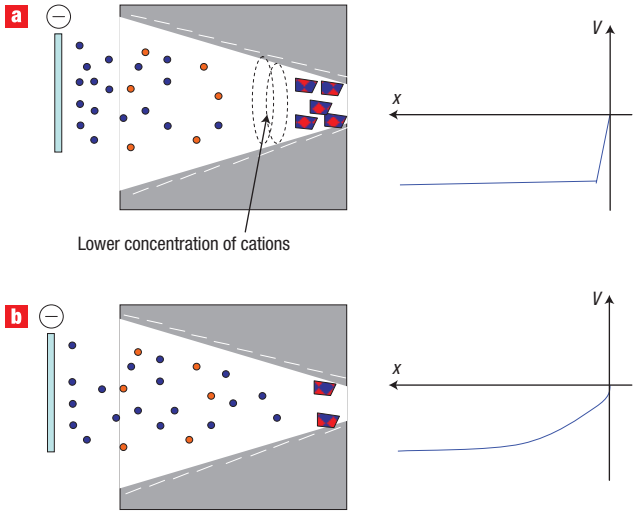

Figure 5 Scheme of the transient formation of the nanoprecipitates. The formation of nanocrystals causes the local cation concentrations next to the precipitate to be reduced due to (1) a lower electric potential in the region adjacent to the precipitate, (2) the cations being driven out of the pore by the electric field, (3) the precipitation hindering the addition of cations into the pore, and (4) the diffusion of ions into the bulk where the ionic concentrations are higher. **a**, Lowering of cation concentrations favours dissolution of the nanoprecipitate. **b**, The nanoprecipitate plug is broken up and the current flow resumes. The panels on the right-hand side schematically show the distribution of transmembrane potential inside the nanopore with and without the precipitate plug.

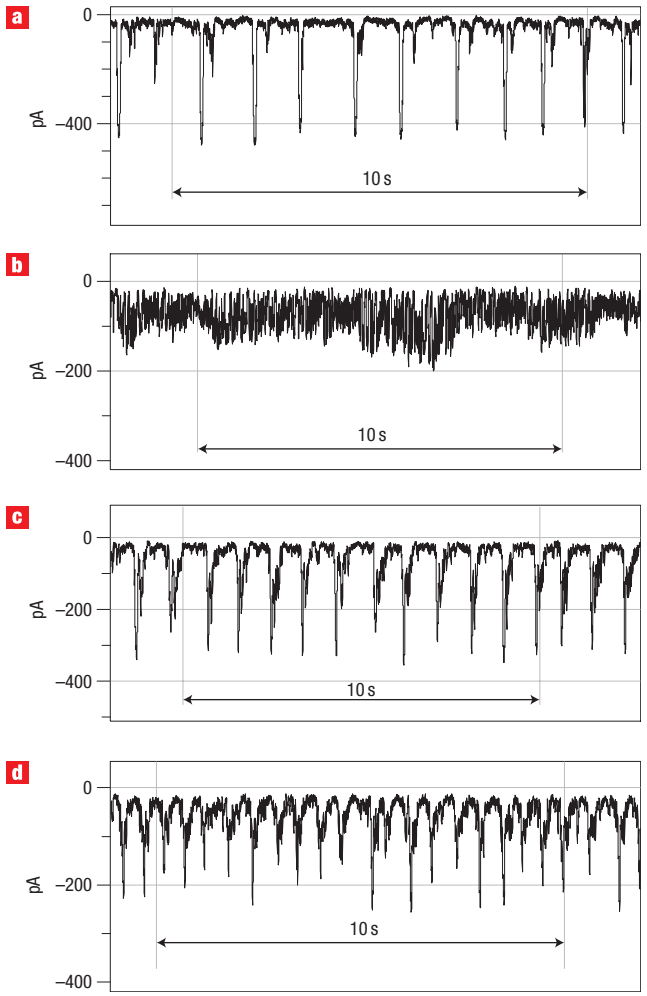

Figure 6 Influence of biomolecules on the signature of the ion current oscillations recorded in 0.1 M KCl, 0.2 mM $CoCl_2$ and 2 mM pH 8 phosphate buffer. a, 'Control' recordings of ion current through a single nanopore with a tip opening of 3 nm in diameter. **b**, Addition of 15 μM neomycin breaks down the $CoHPO_4$ oscillations shown in **a**. **c**, Addition of 15 μM spermine increases the frequency of current oscillations observed with $CoHPO_4$. The frequency of oscillations increases with increased concentrations of spermine. **d**, Recordings with 30 μM spermine.

that is, the ion current signals in 0.1 M KCl after adding neomycin did not differ significantly from the control recordings (see Supplementary Information, Fig. S12).

Future studies will be focused on investigating the details of the sensing mechanism of this stochastic sensor. Our first results indicate that the molecules are detected as they disturb the nanoprecipitation process occurring at the pore tip. Because the tip of the pore has a sub-femtolitre volume, we expect the sensing to be sensitive down to a single molecule in a manner similar to that reported for protein nanopores[33]. Similarly to the response of the protein-based pore, the frequency shift of the oscillating signal in our nanopores can be related to the concentration of an analyte, and its nature could be identified through variation in the shape of the pulse.

$CaHPO_4$ has attracted a great deal of scientific interest because of its biological role in biomineralization processes. This compound is thought to be one of the precursors of hydroxyapatite, which is the major component of vertebrate hard tissues such as bone and teeth. Magnesium hydroxide is popularly known as milk of magnesia. The striking difference between the ion current signature obtained with magnesium hydroxide and calcium hydrogen phosphates could be attributed to the differences in crystal structure of these two materials. Magnesium hydroxide crystals are known to consist of octahedron sheets that do not have residual charges[34], and the sheets are therefore not connected to each other by ionic bonds but rather by weak residual interactions. In contrast, $CaHPO_4$ crystals have a fully ionic character[35]. Moreover, calcium ions in the $CaHPO_4$ lattice have two kinds of coordination with seven or eight nearest oxygen neighbours. The ionic type of the crystal, the differences in its structure, and its interactions with the pore walls are expected to influence its stability and its dissolution kinetics in high electric fields.

We should also point out that our system of single nanopores in contact with an undersaturated solution of a weakly soluble compound gives a unique insight into the kinetics of the earliest stages of crystallization. This might lead to useful practical advances such as the formation of crystals of proteins. As the pore volume at the tip is very small, each ion current decrease we observe in the time series probably corresponds to one or several crystallization nucleation sites forming in the pore.

CONCLUSIONS

We have presented a system of a single nanopore in which negative incremental resistance and ion current oscillations were induced by nanoprecipitation forming in the pore. Our future efforts will focus on the modelling of these current instabilities and relating

them to processes occurring inside the nanopore. We will use the Maxwell–Stefan approach to account for interactions between different species in restricted geometries and to calculate their diffusion coefficients[36]. The presented nonlinear electrochemical system can serve as a model for studying nonlinear phenomena in solution, as a basis for a stochastic sensor, and as a system providing information on the kinetics of the early stages of crystallization.

METHODS

PREPARATION OF SINGLE CONICAL NANOPORES

Foils of polyethylene terephthalate (12 μm thick) were irradiated with single swift heavy ions at the Gesellschaft für Schwerionenforschung in Darmstadt, Germany. The irradiated foils were subsequently etched from one side with 9 M NaOH while the other side of the membrane was in contact with an acidic stopping solution[20]. This asymmetric etching process led to the formation of conically shaped nanopores. The diameter of the large pore opening, called the base, was estimated on the basis of the bulk etch rate, which for PET with 9 M NaOH, and at room temperature, is 2.13 nm min^{-1} (ref. 20). The diameter of the small opening, called the tip, was measured by the electrochemical method described previously[20,25].

RECORDINGS OF ION CURRENT THROUGH SINGLE-PORE POLYMER MEMBRANES

A single-pore polymer membrane was inserted between two chambers of a conductivity cell[20]. We used Ag/AgCl electrodes (Bioanalytical Systems) containing a saturated KCl solution and home-made Ag/AgCl electrodes for measuring transmembrane ion currents. The potential differences were computed as $V_b - V_t$, where V_b and V_t are the potentials on the electrodes at the base and the tip side, respectively. Positive currents in this electrode configuration indicate that cations are flowing from the base to the tip. The ion currents were recorded with the Axopatch 200B amplifier (Molecular Devices) in voltage-clamp mode using a low-pass Bessel filter of 2 kHz. The signal was digitized with a Digidata 1322 A (Molecular Devices) at 10 kHz, and viewed with the Clampex 9.2 software (Molecular Devices). We typically recorded 2-min ion current measurements at constant voltages sweeping from +1 V to −1 V at 100 mV increments.

All ion current recordings were performed with 0.1 M KCl as the background electrolyte with various sub-millimolar and millimolar concentrations of Mg^{2+}, Ca^{2+} or Co^{2+}. In some cases, pH 8 phosphate buffer (PBS) was used by combining a specific ratio of 5% potassium dihydrogen phosphate (KH_2PO_4) and 95% potassium hydrogen phosphate (K_2HPO_4). Higher pH values of pH 9.5 were adjusted with 2 mM 3-(cyclohexylamino)-2-hydroxy-1-propanesulphonic acid (CAPSO) buffer.

DATA ANALYSIS

Analysis of ion current signals was performed using Matlab 7.2 and Clampfit 9.2.

Received 22 August 2007; accepted 23 November 2007; published 23 December 2007.

References

1. Ashcroft, F. M. *Ion Channels and Disease* (Academic Press, New York, 1999).
2. Eisenberg, R. S. Atomic biology, electrostatics and ionic channels. In *New Developments and Theoretical Studies of Proteins* Vol. 7 (ed. Elber, R.) Ch. 5, 269–357, *Advanced Series in Physical Chemistry* (World Scientific, Philadelphia, 1996).
3. Eisenberg, R. S. Ionic channels as natural nanodevices. *J. Comp. Electr.* **1,** 331–334 (2002).
4. Kasianowicz, J. J., Brandin, E., Branton, D. & Deamer, D. W. Characterization of individual polynucleotide molecules using a membrane channel. *Proc. Natl Acad. Sci. USA* **93,** 13770–13773 (1996).
5. Bayley, H. & Martin, C. R. Resistive-pulse sensing—from microbes to molecules. *Chem. Rev.* **100,** 2575–2594 (2000).
6. Dekker, C. Solid-state nanopores. *Nature Nanotech.* **2,** 209–215 (2007).
7. Uram, J. D., Ke, K., Hunt, A. J. & Mayer, M. Submicrometer pore-based characterization and quantification of antibody–virus interactions. *Small* **2,** 967–972 (2006).
8. Iqbal, S. M., Akin, D. & Bashir, R. Solid-state nanopore channels with DNA selectivity. *Nature Nanotech.* **2,** 243–248 (2007).
9. Berezhkovskii, A. M., Hummer, G. & Bezrukov, S. M. Identity of distributions of direct uphill and downhill translocation times for particles traversing membrane channels. *Phys. Rev. Lett.* **97,** 020601 (2006).
10. Muthukumar, M. Polymer escape through a nanopore. *J. Chem. Phys.* **118,** 5174–5184 (2003).
11. Keyser, U. F. *et al.* Direct force measurements on DNA in a solid-state nanopore. *Nature Phys.* **2,** 473–477 (2006).
12. Stein, D., Kruithof, M. & Dekker, C. Surface-charge-governed ion transport in nanofluidic channels. *Phys. Rev. Lett.* **93,** 035901 (2004).
13. Israelachvili, J. *Intermolecular and Surface Forces* 2nd edn (Academic Press, London, 1991).
14. Daiguji, H., Yang, P. & Majumdar, A. Ion transport in nanofluidic channels. *Nano Lett.* **4,** 137–142 (2004).
15. Vlassiouk, I. & Siwy, Z. Nanofluidic diode. *Nano Lett.* **7,** 552–556 (2007).
16. Karnik, R., Duan, C., Castelino, K., Daiguji, H. & Majumdar, A. Rectification of ionic current in a nanofluidic diode. *Nano Lett.* **7,** 547–551 (2007).
17. Karnik, R. *et al.* Electrostatic control of ions and molecules in nanofluidic transistors. *Nano Lett.* **5,** 943–948 (2005).
18. Eisenberg, R. S. Computing the field in proteins and channels. *J. Membrane Biol.* **150,** 1–25 (1996).
19. Fleischer, R. L., Price, P. B. & Walker, R. M. *Nuclear Tracks in Solids. Principles and Applications* (Univ. of California Press, Berkeley, 1975).
20. Apel A., Korchev Y. E., Siwy Z., Spohr R. & Yoshida M. Diode-like single-ion track membrane prepared by electro-stopping. *Nucl. Instrum. Methods Phys. Res. B* **184,** 337–346 (2001).
21. Siwy, Z., Powell, M. R., Kalman, E., Astumian, R. D. & Eisenberg, R. S. Negative incremental resistance induced by calcium in asymmetric nanopores. *Nano Lett.* **6,** 473–477 (2006).
22. Siwy, Z. *et al.* Calcium-induced voltage gating in single conical nanopores. *Nano Lett.* **6,** 1729–1734 (2006).
23. Dean, J. A. *Lange's Handbook of Chemistry* 15th edn (McGraw-Hill, New York, 1999).
24. Cervera, J., Schiedt, B. & Ramirez, P. A Poisson/Nernst–Planck model for ionic transport through synthetic conical nanopores. *Europhys. Lett.* **71,** 35–41 (2005).
25. Siwy Z. & Fulinski A. Fabrication of a synthetic nanopore ion-pump. *Phys. Rev. Lett.* **89,** 198103 (2002).
26. Ciavatti, L. The Specific Interaction Theory in equilibrium analysis. Some empirical rules for estimating interaction coefficients of metal ion complexes. *Anali di Chimica by Societa Chimica Italiana* **80,** 255–263 (1990).
27. Ciavatti, L. The Specific Interaction Theory in evaluating ionic equilibria. *Anali di Chimica by Societa Chimica Italiana* **80,** 551–567 (1980)
28. Nonner, W. & Eisenberg, R. S. Ion permeation and glutamate residues linked by Poisson–Nernst–Planck theory in L-type calcium channels. *Biophys. J.* **75,** 1287–1305 (1998).
29. Constantin, D. & Siwy, Z. Poisson–Nernst–Planck model of ion current rectification through a nanofluidic diode. *Phys. Rev. E* **76,** 041202 (2007).
30. Krischer, K., Mazouz, N. & Grauel, P. Fronts, waves, and stationary patterns in electrochemical systems. *Angew. Chem. Int. Edn* **40,** 850–859 (2001).
31. Kurin-Csörgei, K., Epstein, I. R. & Orban, M. Systematic design of chemical oscillators using complexation and precipitation equilibria. *Nature* **433,** 139–142 (2005).
32. Epstein I. R. & Pojman, J. A. *Introduction to Nonlinear Chemical Dynamics. Oscillations, Waves, Patterns and Chaos* (Oxford Univ. Press, New York, 1998).
33. Bayley, H. & Cremer, P. S. Stochastic sensors inspired by biology. *Nature* **413,** 226–230 (2001).
34. Brindley, G. W. & Kao, C-C. Structural and IR relations among brucite-like divalent metal hydroxides. *Phys. Chem. Minerals* **10,** 187–191 (1984).
35. Dickens, B., Bowen, J. S. & Brown, W. E. A refinement of the crystal structure of $CaHPO_4$ (synthetic monetite). *Acta Cryst.* **B28,** 797–806 (1971).
36. Krishna, R. & Wesselingh, J. A. The Maxwell–Stefan approach to mass transfer. *Chem. Eng. Sci.* **52,** 861–911 (1997).

Acknowledgements

Irradiation with swift heavy ions was performed at the Gesellschaft für Schwerionenforschung (GSI), Darmstadt, Germany. We thank the Alfred P. Sloan Foundation, the IM-SURE undergraduate programme, the Institute for Surface and Interface Science and the Institute for Complex Adaptive Matter for financial support.

Correspondence and requests for materials should be addressed to Z.S.

Supplementary information accompanies this paper on www.nature.com/naturenanotechnology.

Author contributions

Z.S., R.S.E. and I.V. conceived the experiments. M.R.P., M.S. and I.V. performed the experiments. D.C. analysed the data and was in charge of calculations. M.R.P. and Z.S. wrote the manuscript. R.S. co-wrote the manuscript. O.S. and C.C.M. analysed the data, discussed the results, explained the transient character of precipitation formation, and co-wrote the manuscript.